Dopants and Defects in InN and InGaN Alloys

W. Walukiewicz[a,*], R. E. Jones[a,b], S. X. Li[a,b], K. M. Yu[a], J. W. Ager III[a], E. E. Haller[a,b], H. Lu[c] and W. J. Schaff[c]

[a] *Materials Sciences Division, Lawrence Berkeley National Laboratory, Berkeley, CA 94720, USA*

[b] *Department of Materials Science and Engineering, University of California, Berkeley, CA 94720, USA*

[c] *Department of Electrical and Computer Engineering, Cornell University, Ithaca, NY 14853, USA*

** Corresponding author: w_walukiewicz@lbl.gov, 1 510 486 5329 (tel), 1 510 486 5530 (fax)*

Abstract

We have performed systematic studies of the effects of high-energy particle irradiation on the properties of InGaN alloys. In agreement with the amphoteric defect model, irradiation of InN produces donor-like defects. . The electron concentration increases with increasing radiation dose and saturates at $4x10^{20}$ cm^{-3} at very high doses. We find that the increase of the electron concentration causes a large blue-shift of the absorption edge, which is well-explained by the Burstein-Moss effect. The maximum electron concentration decreases with increasing Ga fraction in irradiated $In_{1-x}Ga_xN$ alloys as the conduction band edge approaches the Fermi level stabilization energy (E_{FS}). For $x > 0.66$ the conduction band edge moves above E_{FS} and the irradiation of n-type films produces acceptor-like defects, resulting in a reduced free electron concentration. An analysis of the concentration dependence of the electron mobility in InN indicates that the dominant defects in irradiated InN are triply-charged donors. Finally, we show that InN films doped with Mg acceptors behave like undoped films above a threshold radiation dose.

Keywords: A1. Defects, A1. Doping, B1. Nitrides, B2. Semiconducting indium compounds

PACS numbers: 61.80.-x, 71.55.Eq, 72.10.Fd, 78.66.Fd

1. Introduction

Indium Nitride (InN) exhibits a strong propensity for n-type doping. All films grown to date have shown n-type conductivity with free electron concentrations ranging from mid-10^{17} cm^{-3} to 10^{21} cm^{-3} [1]. This spread of electron concentrations leads to a large variation in the energy of the optical absorption edge known as the Burstein-Moss shift [2, 3]. While impurity atoms were first thought to be the cause of the high electron concentrations, secondary ion mass spectroscopy has shown that their concentrations cannot always account for the free electrons [3]. Instead, the seemingly inherent proclivity for n-type conductivity can be attributed to the location of the Fermi stabilization energy (E_{FS}) high in the conduction band of InN, such that native defects are primarily donor-like, as explained by the amphoteric defect model (ADM) [4, 5].

According to the ADM, the formation energy of a native defect is dependent on the location of the Fermi level (E_F) with respect to the Fermi stabilization energy (E_{FS}), which is the average energy level of native defects. The formation energy of donor-like (acceptor-like) defects decreases for $E_F < E_{FS}$ ($E_F > E_{FS}$). When defects are formed in a material, E_F moves toward E_{FS}, eventually pinning E_F at E_{FS} with the formation of donor and acceptor defects at equal rates.

Thus, native point defects play a critical role in determining the properties of InN. To better understand this role, we subjected InN, as well as $In_{1-x}Ga_xN$, films to irradiation with energetic electrons, protons and He^+ ions. We show that for $x \leq 0.6$, the radiation-induced defects behave as donors, and that irradiation at high doses can be used to control the electronic

and optical properties of InN and $In_{1-x}Ga_xN$ films. In addition, we construct a detailed model for electron transport in InN that accounts for the nonparabolicity of the conduction band that results from the k • p interaction with the light-hole band across the narrow bandgap [2].

2. Experimental

InN and $In_{1-x}Ga_xN$ films (x = 0.3, 0.6) were grown by molecular-beam epitaxy or migration-enhanced epitaxy on c-sapphire substrates with a GaN or AlN buffer layer [6]. The thickness of the films ranged from 100 to 7000 nm. Most films were not intentionally doped (i.e., "undoped"); three InN films were doped with magnesium. Free electron concentrations in the as-grown, undoped films were between $3x10^{17}$ and $8x10^{19}$ cm^{-3}, and electron mobility values ranged from 2200 to 16 cm^2/V s. Initial free electron concentrations and mobilities in the Mg-doped films ranged from $3x10^{18}$ to $1x10^{19}$ cm^{-3} and 57 to 27 cm^2/V s, respectively. GaN samples (3 μm thick) were grown on c-sapphire by metalorganic chemical vapor deposition (MOCVD). The free electron concentration and mobility of these n-type GaN films were $7.7\times10^{17}/cm^3$ and 190 $cm^2/V\cdot s$, respectively.

Free carrier concentration and mobility were measured with a Hall effect system using a 3000 Gauss magnet. Indium contacts were applied in van der Pauw configuration. Optical absorption measurements were performed at room temperature using a CARY-2390 NIR-VIS-UV spectrophotometer.

High-energy proton (H^+) and helium (He^+) particle irradiation studies used a 2 MeV ion beam generated by a Van de Graaff accelerator. The ion fluences ranged from $1.1x10^{14}$ to $2.7x10^{16}$ cm^{-2}. Irradiation with 1 MeV electrons to fluences between $5x10^{15}$ and $1x10^{17}$ cm^{-2} was

performed at the Dynamitron Electron Accelerator at Kirkland Air Force Base in Albuquerque, New Mexico.

The displacement damage dose (D_d) methodology for modeling the degradation of solar cell performance in outer space, developed by the Naval Research Laboratory, was employed to relate the amount of damage caused by the different types of particles [7, 8]. D_d is the product of the particle fluence, and the Non-Ionizing Energy Loss (NIEL), which is determined by the particle energy and the host material. The NIEL for electrons was estimated from that published for GaAs [8], and the Stopping Power and Range of Ions in Matters (SRIM) program [9] was used for H^+ and He^+ particles. D_d ranged from $1.5x10^{11}$ to $1.8x10^{16}$ MeV/g in our studies. In some cases the same sample was sequentially irradiated to higher doses in order to eliminate any effects of inhomogeneity among samples. The ion penetration depth was calculated to be greater than the film thickness in nearly all samples, causing approximately uniform damage with film depth, and leaving the end-of-range damage in the sapphire substrate. Ion channeling spectroscopy verified that the films remained single crystalline after irradiation. For example, the minimum yield, χ, increased from 0.04 in an as-grown InN sample to only 0.11 after He^+ irradiation with the highest dose of 1.8×10^{16} MeV/g.

3. Defect doping

In Figure 1 the electron concentration in irradiated, undoped InN is plotted as a function of displacement damage dose (D_d). The figure shows that the irradiation introduces electrically-active donor defects. The increase in electron concentration is approximately linear with dose for each type of particle, and thus irradiation provides a method for controlled n-type doping of

InN over a wide concentration range. For D_d of 5.9×10^{15} MeV/g and higher, however, the electron concentration saturates at roughly 4×10^{20} cm^{-3}.

This behavior is well-explained by the amphoteric defect model (ADM) [4]. Because E_{FS} is located high in the conduction band in InN [5], the radiation-induced native defects are primarily donor-like. As the electron concentration increases, though, E_F moves towards E_{FS}. Once E_F reaches E_{FS}, donor and acceptor defects are formed at equal rates, pinning E_F at E_{FS} and resulting in a saturation of the electron concentration. We calculated this saturation concentration (N_S) by setting $E_F = E_{FS}$, while accounting for the nonparabolicity of the conduction band as well as the bandgap renormalization effect [10]. N_S (shown as dashed lines in Fig. 1) agrees well with the experimental data.

Additional proof of the validity of the ADM comes from the behavior upon irradiation of two $In_{1-x}Ga_xN$ samples and one GaN sample with similar initial electron concentrations to the InN sample (Fig. 1). The electron concentrations in the two $In_{1-x}Ga_xN$ (x = 0.3, 0.6) films increase with irradiation toward a saturation value (N_S, see Fig. 1), as in InN. However, the radiation doping effect is less pronounced as x increases, since the conduction band edge moves closer to E_{FS}. The conduction band edge reaches E_{FS} for $x \sim 0.66$. Thus, the Fermi energy is pinned at a lower energy with respect to the conduction band edge as x increases, and N_S decreases correspondingly. In GaN, E_{FS} is located 0.7 eV below the conduction band edge [5]. Therefore, irradiation of n-type GaN ($E_F > E_{FS}$), produces acceptor-like defects that compensate the material, eventually making it highly resistive.

Further evidence for n-type, radiation-defect doping of InN and In-rich $In_{1-x}Ga_xN$ comes from a study of the effects of 2 MeV He^+ irradiation on the optical absorption edge [11]. The inset of Fig. 2 shows the monotonically-increasing blue shift of the absorption edge in InN with

increasing He^+ particle dose. This effect is due to the Burstein-Moss shift as the conduction band states fill with electrons from the additional donor defects. The Fermi energy (E_F) was determined for each spectrum by numerical fitting (also shown) using a Gaussian broadening parameter. The values of E_F are consistent with those calculated from the electron concentrations measured by Hall effect [11]. The highest E_F values correspond to the saturation of the electron concentration when E_F reaches E_{FS}. This blue shift of the absorption edge is also seen for $In_{1-x}Ga_xN$ films with $x < 0.66$ (not shown), and the amount of the shift decreases with increasing x, corresponding to the lower values of N_S [5].

In contrast, the absorption edge in GaN (Fig. 2) is unaffected by 2 MeV He^+ irradiation. Instead, a sub-bandgap absorption feature appears at ~2.7 eV, and grows in magnitude with increasing irradiation dose. This observation is fully consistent with the ADM that predicts the formation of acceptor-like defect levels at E_{FS}, which is located 2.7 eV above the valence band edge.

4. Electron Mobility

In addition to controlling the electron concentration, we find that energetic particle irradiation is a reliable method for controlling electron mobility in InN [12]. The inset in Fig. 3 shows electron mobility plotted as a function of electron concentration for as-grown InN films; the main figure depicts this data for films irradiated with H^+ and He^+ particles. While there is a large spread in the data of the as-grown samples, there is a well-defined relationship between electron concentration and mobility in irradiated samples across the entire concentration range of almost three orders of magnitude. The scatter in the as-grown samples reflects differences in quality among InN films and may be attributable to surface effects, scattering by dislocations

[13] and three-dimensional defects, and differences in the degree of crystallinity of the films. Irradiation of these different films homogenizes their transport properties with respect to the radiation dose, and allows for an in-depth study of the factors limiting electron mobility in irradiated samples.

We have performed theoretical calculations of electron mobility in irradiated samples for the entire span of electron concentrations we can achieve with radiation doping (i.e., 10^{18} to 10^{20} cm^{-3}). Preliminary calculations assuming a parabolic band structure with a band-edge effective mass of $0.7m_0$ determined that scattering by ionized defects is the dominant factor limiting electron mobility across the entire concentration range. Phonon scattering mechanisms (including optical, acoustic deformation potential and acoustic piezoelectric) were found to be largely insignificant, although optical phonon scattering does play some role at the lowest electron concentrations (i.e., low 10^{18} cm^{-3}) [13]. We will therefore focus below on ionized defect scattering, and present more thorough calculations of electron mobility that account for the effects of a nonparabolic conduction band. The parameters used in these calculations are listed in Table I.

To properly describe the conduction band structure over the wide range in energy of states occupied at these high electron concentrations, we needed to account for the k • p interaction between the conduction band and the light-hole band across the narrow bandgap. This interaction creates an energy-dependent electron effective mass while also reducing the electron scattering between conduction band states due to the decreased overlap between electron wavefunctions. In our calculations, we employed Kane's two-band model [14], which gives mixed-symmetry conduction band states. The nonparabolic dispersion relation is:

$$E(k) = -\frac{E_g}{2} + \left[\left(\frac{E_g}{2}\right)^2 + \frac{E_g \hbar^2 k^2}{2m_0^*}\right]^{1/2} + \frac{\hbar^2 k^2}{2m_0}, \qquad (1)$$

where m_0^* is the electron effective mass at the conduction band edge, to which point the energy is referenced. The resulting equation for electron mobility limited only by ionized center scattering is derived from the work of Zawadzki and Szymanska on InSb, another narrow gap semiconductor [15]. It is given by:

$$\mu_i(k) = \frac{\chi_0^2}{2\pi e^3 \hbar Z^2 N_i F_i} \left(\frac{dE}{dk} \right)^2 k \,, \qquad (2)$$

where χ_0 is the static dielectric constant, Z is the charge of the ionized defect centers, N_i is the concentration of ionized (defect) centers, and F_i is a function that takes into account free electron screening effects and the reduction of the scattering rates that result from the mixed nature of the conduction band wavefunctions [15]. We averaged this energy-dependent electron mobility (μ_i) with the Fermi-Dirac distribution function over all of the conduction band states to get the macroscopic electron mobility for a given electron concentration.

The theoretical, macroscopic electron mobility is plotted as a function of electron concentration for the cases of singly-charged (Z=1), ionized donor defects with no compensation (θ=0), with a constant compensation ratio of 0.5, and with a constant compensation ratio of 0.6 (Fig. 3). For these situations, N_i is given by:

$$N_i = \frac{n(1+\theta)}{(1-\theta)} \,, \qquad (3)$$

where n is the free electron concentration. The values for θ = 0.5 are equivalent to those for the case of triply-charged donor defects (Z=3, N_i=n/Z) with θ = 0. It is apparent that the lines for compensated or triply-charged donor defects are much better fits to the experimental data; the values for singly-charged, uncompensated defects are about a factor of four too high. Although the calculated mobility with θ=0.6 fits the experimental data very well, we know from the ADM that it is unlikely that irradiation could produce a constant compensation ratio that does not

depend on E_F, and therefore electron concentration. Thus, it is most probable that the native defects formed by high-energy irradiation are triply-charged donors.

In this treatment, we have not considered short-range scattering by the ionized defects. This mechanism seems to become significant at high electron concentrations, and it should be included in future calculations. Scattering by dislocations and three-dimensional defects is not believed to play a large role in limiting the mobility of irradiated samples, as transmission electron microscopy (TEM) studies have shown that energetic particle irradiation does not increase the concentration of dislocations [16].

5. Magnesium-doped InN

We have shown recently that doping with Mg strongly affects the electronic and optical properties of InN [17]. The effects of the doping can be understood by assuming that the properties of InN:Mg films are determined by the contributions from a p-type bulk and an n-type surface inversion layer. To further confirm these assertions we have used He^+-particle irradiation to introduce donor defects into Mg-doped films, and thereby transform the bulk material to n-type. Figure 4 shows the electron concentration as a function of D_d in three Mg-doped films and one undoped InN film. In each of the Mg-doped films, there was a threshold below which the 2 MeV He^+ irradiation did not have much effect on the transport properties measured by Hall effect. However, for D_d above approximately 10^{15} MeV/g, the electron concentrations in the Mg-doped films are comparable to those of the undoped sample. Similarly, the electron mobilities of Mg-doped samples irradiated above this dose approach the values for undoped InN (Fig. 3).

These results are in good agreement with the assumption that the electrical properties of as-grown or lightly-irradiated samples are determined by the transport in the n-type inversion layer without any contribution from the electrically-isolated, p-type bulk. At high enough irradiation doses, the donor defects overcompensate the Mg acceptors and the bulk material becomes n-type. This conversion is associated with an increase in the measured electron concentration and electron mobility of the film, because of the added contribution of the bulk layer to the Hall effect measurements [17]. Electron mobility in the bulk is initially higher than mobility at the surface, due to a lower concentration of ionized defect scattering centers. At even higher irradiation doses that generate donor-defect concentrations much greater than the Mg-acceptor concentration, the Mg-doped samples start to behave as irradiated n-type samples, with properties controlled by the radiation-generated donors. We note that the presence of free holes in the bulk layer of Mg-doped InN has not been demonstrated, and so the conductivity of the bulk layer is not known. It remains to be determined whether Mg is a deep or shallow acceptor in InN.

6. Conclusions

We have used Hall effect measurements of electron transport properties and optical absorption measurements to demonstrate that energetic particle irradiation is a reliable method for controlling electrical and optical properties of $In_{1-x}Ga_xN$. This control extends to InN films doped with Mg above a threshold radiation dose (~10^{15} MeV/g). Energetic particle irradiation is an n-type doping method in InN and In-rich InGaN, but forms compensating acceptor defects in n-type GaN, due to the location of E_{FS} relative to the conduction band edge.

Acknowledgments

We thank W. Kemp of the Air Force Research Laboratory, Kirtland Air Force Base for performing the electron irradiation and D. Senft for helpful discussions. We also thank Mr. Milton Yeh of Blue Photonics Inc. for providing the GaN samples. This work is supported by the Director, Office of Science, Office of Basic Energy Sciences, Division of Materials Sciences and Engineering, of the U.S. Department of Energy under Contract No. DE-AC03-76SF00098. The work at Cornell University is supported by ONR under contract NO. N000149910936.

References

[1] K. S. A. Butcher and T. L. Tansley, Superl. and Microstr. 38 (2005) 1.

[2] J. Wu, W. Walukiewicz, Superl. and Microstr. 34 (2003) 63.

[3] J. Wu, W. Walukiewicz, S.X. Li, R. Armitage, J.C. Ho, E.R. Weber, E.E. Haller, H. Lu, W.J. Schaff, A. Barcz, and R. Jakiela, Appl. Phys. Lett. 84 (2004) 2805.

[4] W. Walukiewicz, Physica B, 302 (2001) 123.

[5] S. X. Li, K. M. Yu, J. Wu, R. E. Jones, W. Walukiewicz, J. W. Ager III, W. Shan, E. E. Haller, H. Lu, and W. J. Schaff, Phys. Rev. B 71 (16) (2005) 161201.

[6] H. Lu, W. J. Schaff, J. Hwang, H. Wu, W. Yeo, A. Pharkya, and L. F. Eastman, Appl. Phys. Lett. 77 (2000) 2548.

[7] S. R. Messenger, E. A. Burke, G. P. Summers, M. A. Xapsos, R. J. Walters, E. M. Jackson, and B. D. Weaver, IEEE Trans. Nuclear Sci. 46 (1999) 1595.

[8] S. R. Messenger, G. P. Summers, E. A. Burke, R. J. Walters, and M. A. Xapsos, Prog. Photovolt: Res. Appl. 9 (2000) 103.

[9] J. F. Ziegler, J. P. Biersack, and U. Littmark, The Stopping and Range of Ions in Solids, vol. 1, Pergamon Press, New York, 1985.

[10] J. Wu, W. Walukiewicz, W. Shan, K. M. Yu, J. W. Ager III, E. E. Haller, Hai Lu, and William J. Schaff, Phys. Rev. B 66 (2002) 201403.

[11] S. X. Li, E.E. Haller, K. M. Yu, W. Walukiewicz, J. W. Ager III, J. Wu, and W. Shan, H. Lu and W. J. Schaff, Appl. Phys. Lett. 87 (2005) 161905.

[12] R. E. Jones, S. X. Li, L. Hsu, K. M. Yu, W. Walukiewicz, Z. Liliental-Weber, J. W. Ager III, E. E. Haller, H. Lu and W. J. Schaff, Phys. Rev. B (in press).

[13] D. C. Look, H. Lu, W. J. Schaff, J. Jasinski, Z. Liliental-Weber, Appl. Phys. Lett. 80 (2002) 258.

[14] E. O. Kane, J. Phys. Chem. Sol. 1 (1957) 249.

[15] W. Zawadzki and W. Szymanska, Phys. Stat. Sol. (b) 45 (1971) 415.

[16] Z. Liliental-Weber, unpublished (2005).

[17] R.E. Jones, K. M. Yu, S.X. Li, W. Walukiewicz, J.W. Ager III, E.E. Haller, H. Lu, and W. J. Schaff, to be published.

[18] T. Inushima, M. Higashiwaki, T. Matsui, Phys. Rev. B 68 (2003) 235204.

Table I

Parameters used in InN electron mobility calculations

Static dielectric constant, χ_0	10.5 [18]
High frequency dielectric constant	6.7 [18]
Bandgap energy, Eg	0.7 eV
Effective electron mass at CBE, m_0^*	0.07 m_0
Longitudinal optical phonon energy	0.073 eV
Deformation potential	2.5 eV
Acoustic phonon velocity	5.07×10^5 cm/s
Density	6.81 g/cm^3
Piezoelectric constant	4.71×10^7 V/cm

Figure Captions

Fig. 1: Electron concentration as a function of damage displacement dose (D_d) in n-type $In_{1-x}Ga_xN$ films irradiated with electrons, protons and He^+ particles. The calculated saturation concentrations (N_s) are also shown as dashed lines.

Fig. 2: Absorption spectra of as-grown and He^+-irradiated GaN and InN (inset). The 2 MeV He^+ doses are noted. The calculated Fermi level corresponding to each absorption edge in InN is also shown.

Fig. 3: Electron mobility plotted as a function of electron concentration in as-grown InN films (inset) and films irradiated with H^+ and He^+ particles. Both undoped and Mg-doped films are shown, but the irradiated Mg-doped samples are included for $D_d > 1.5 \times 10^{15}$ MeV/g only. The plotted lines are theoretical calculations for the cases of mobility limited by scattering from singly-charged donor defects with compensation ratios of 0, 0.5 (or, equivalently, uncompensated, triply-charged donors) and 0.6.

Fig. 4: Electron concentration plotted as a function of displacement damage dose (D_d) in films irradiated with He^+ particles.

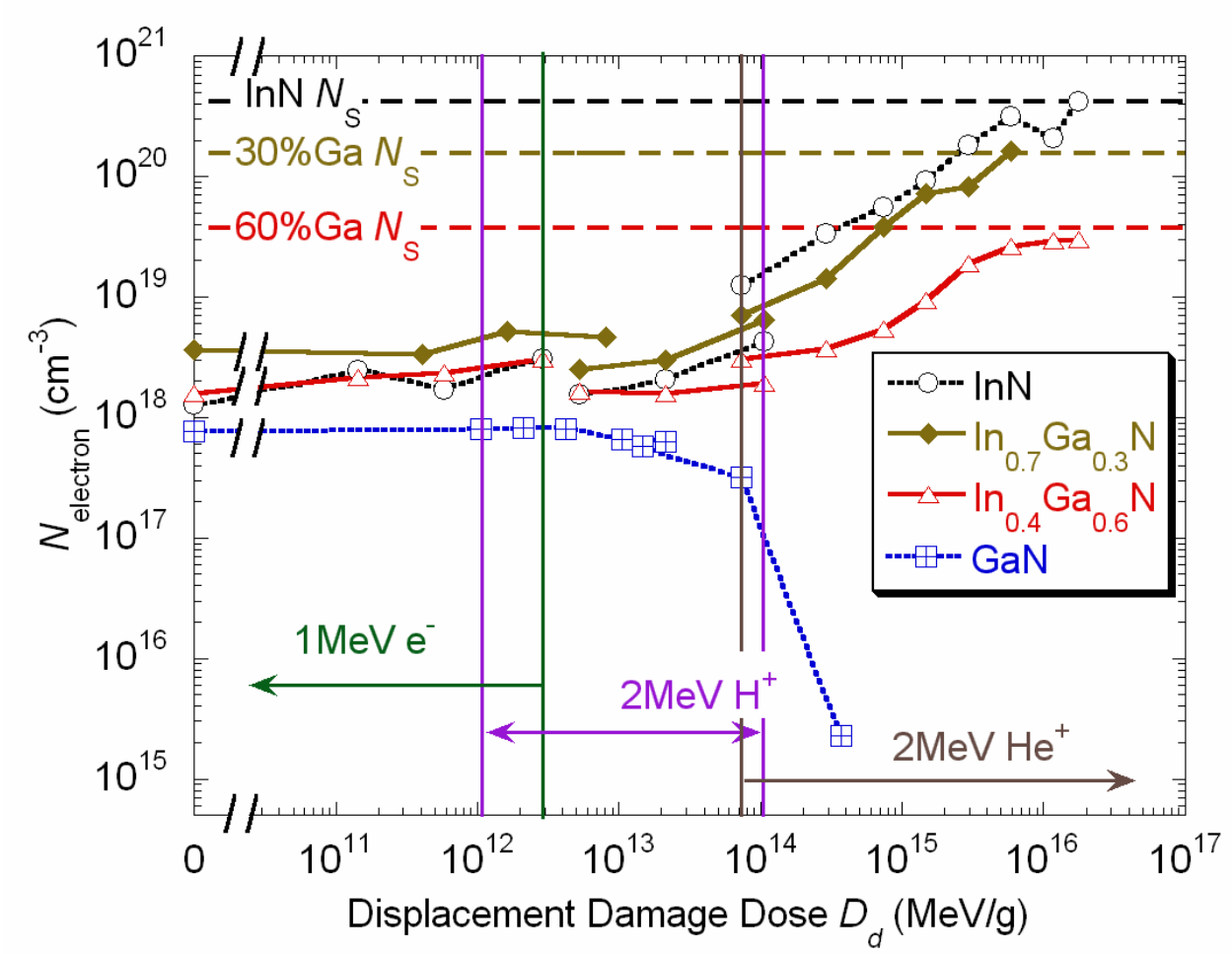
InN N_S
30%Ga N_S
60%Ga N_S
InN
$In_{0.7}Ga_{0.3}N$
$In_{0.4}Ga_{0.6}N$
GaN
1MeV e^-
2MeV H^+
2MeV He^+
$N_{electron}$ (cm^{-3})
Displacement Damage Dose D_d (MeV/g)
10^{21}
10^{20}
10^{19}
10^{18}
10^{17}
10^{16}
10^{15}
0
10^{11}
10^{12}
10^{13}
10^{14}
10^{15}
10^{16}
10^{17}

Figure 1

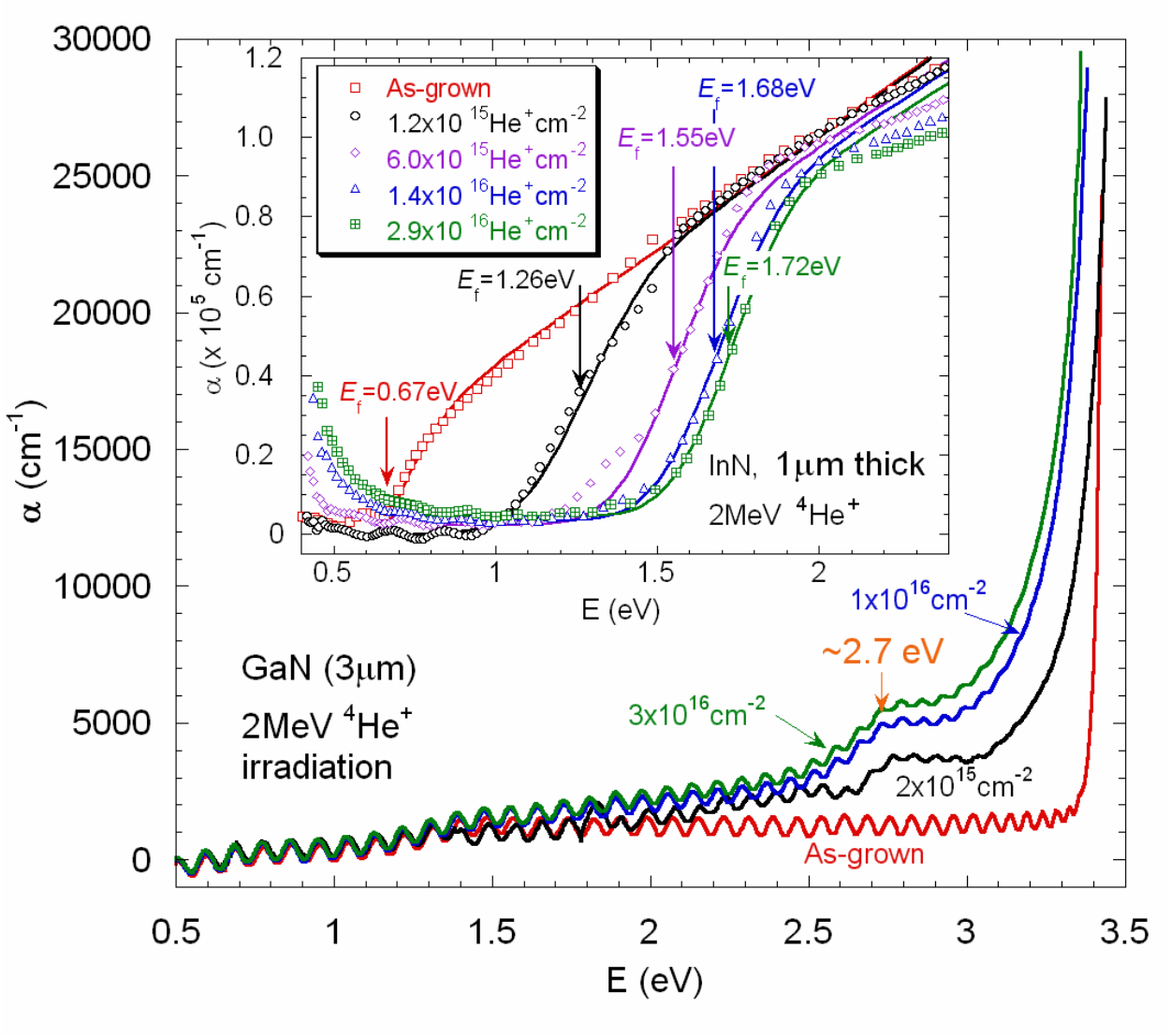
30000
25000
20000
15000
10000
5000
0
α (cm^{-1})
0.5
1
1.5
2
2.5
3
3.5
E (eV)
GaN (3μm)
2MeV ^{4}He$^+$
irradiation
As-grown
2x10^{15}cm^{-2}
3x10^{16}cm^{-2}
1x10^{16}cm^{-2}
~2.7 eV
1.2
1.0
0.8
0.6
0.4
0.2
0
α (x 10^5 cm^{-1})
As-grown
1.2x10 ^{15}He$^+$cm^{-2}
6.0x10 ^{15}He$^+$cm^{-2}
1.4x10 ^{16}He$^+$cm^{-2}
2.9x10 ^{16}He$^+$cm^{-2}
E_f=1.68eV
E_f=1.55eV
E_f=1.72eV
E_f=1.26eV
E_f=0.67eV
InN, 1μm thick
2MeV ^{4}He$^+$
0.5
1
1.5
2
E (eV)

Figure 2

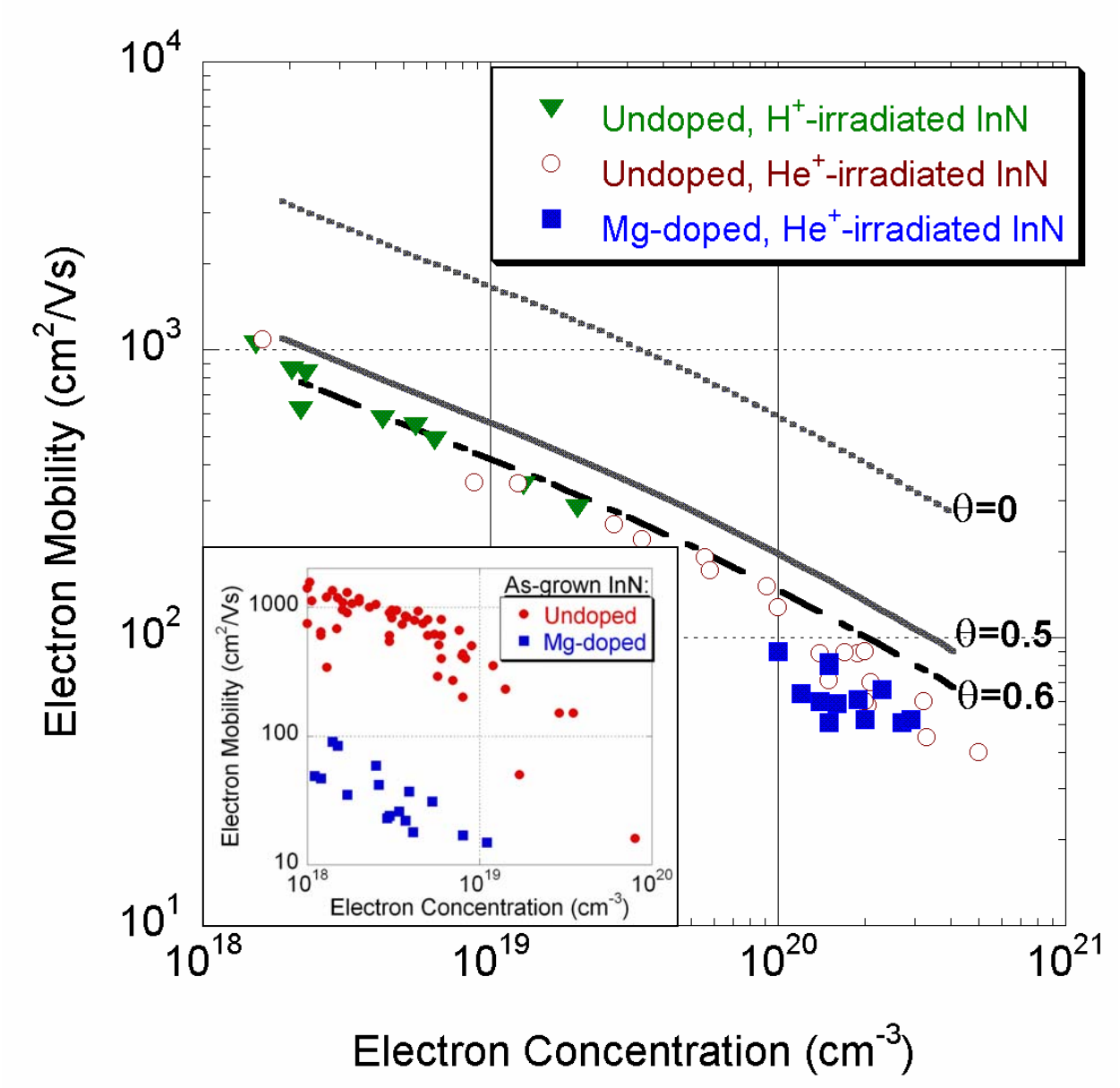
Undoped, H+-irradiated InN
Undoped, He+-irradiated InN
Mg-doped, He+-irradiated InN
θ=0
θ=0.5
θ=0.6
As-grown InN:
Undoped
Mg-doped
Electron Mobility (cm2/Vs)
Electron Concentration (cm-3)
Electron Mobility (cm2/Vs)
Electron Concentration (cm-3)

Figure 3

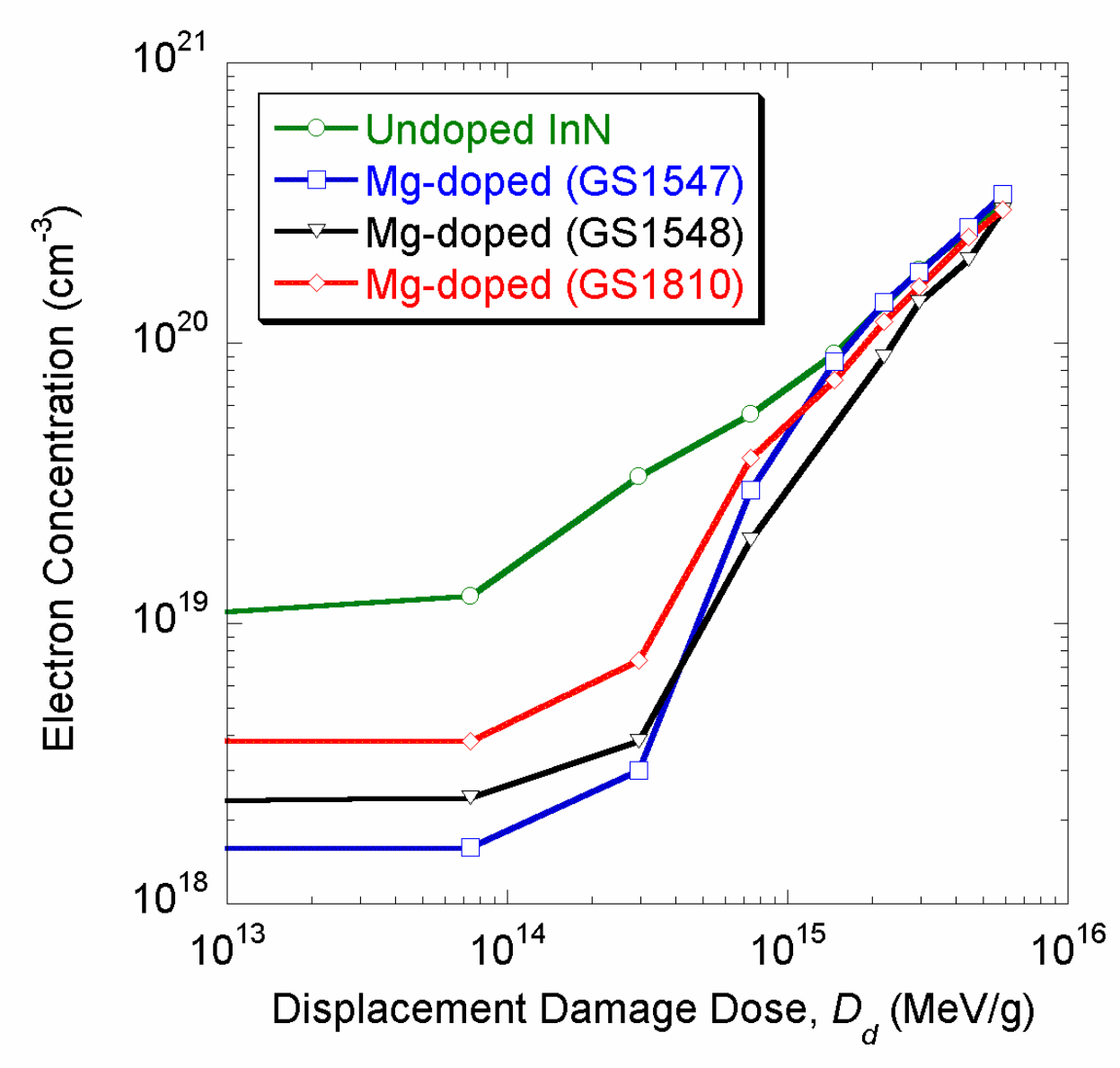
Undoped InN
Mg-doped (GS1547)
Mg-doped (GS1548)
Mg-doped (GS1810)
Electron Concentration (cm-3)
10^21
10^20
10^19
10^18
10^13
10^14
10^15
10^16
Displacement Damage Dose, D_d (MeV/g)

Figure 4